Photofield-Effect in Amorphous InGaZnO TFTs

Tze-Ching Fung[1], Chiao-Shun Chuang[3], Barry G. Mullins[1], Kenji Nomura[2], Toshio Kamiya[2], Han-Ping David Shieh[3], Hideo Hosono[2] and Jerzy Kanicki[1]

[1]Dept. of Electrical Engineering and Computer Science, University of Michigan, Ann Arbor, Michigan 48109, U.S.A.

TEL:001-734-936-0972, e-mail: kanicki@eecs.umich.edu

[2]ERATO-SORST, JST, in Frontier Collaborative Research Center / Material and Structure Lab., Tokyo Institute of Technology 4259 Nagatsuta, Midori-Ku, Yokohama 226-8503, Japan

[3]Dept. of Photonics & Display Institute, National Chiao Tung University, Hsinchu, Taiwan 30010 R.O.C.

Keywords : Metal oxide semiconductor, InGaZnO, TFT, Photofield effect

Abstract

We study the amorphous In-Ga-Zn-O thin-film transistors (TFTs) properties under monochromatic illumination (λ=420nm) with different intensity. TFT off-state drain current (I_{DS_off}) was found to increase with the light intensity while field effect mobility (μ_{eff}) is almost unchanged; only small change was observed for sub-threshold swing (S). Due to photo-generated charge trapping, a negative threshold voltage (V_{th}) shift is also observed. The photofield-effect analysis suggests a highly efficient UV photocurrent conversion in a-IGZO TFT. Finally, a-IGZO mid-gap density-of-states (DOS) was extracted and is more than an order lower than reported value for a-Si:H, which can explain a good switching properties of the a-IGZO TFTs.

1. Introduction

With the high field-effect mobility and excellent switching properties, amorphous In-Ga-Zn-O (a-IGZO) thin film transistor (TFTs) are being considered as possible new material for next generation active-matrix flat panel display (AM-FPD) [1] or imager. Since the TFT pixel electrode circuits for these applications can be exposed to light during operation, study of the a-IGZO TFT photo-electric properties is very important for optimizing future device structure and pixel circuits design.

a-IGZO was found to be highly visible light transparent with optical energy band gap (Tauc gap) of ~3eV [2]. We studied the wavelength dependent a-IGZO TFT photosensitivity under broad-band illumination (λ=365~660nm) and found that the a-IGZO TFT is stable under visible light (λ=460~ 660nm). Under UV illumination (λ<400nm), TFT off-state drain current (I_{DS_off}) increases and the change is consistent with the Tauc gap of the a-IGZO [3].

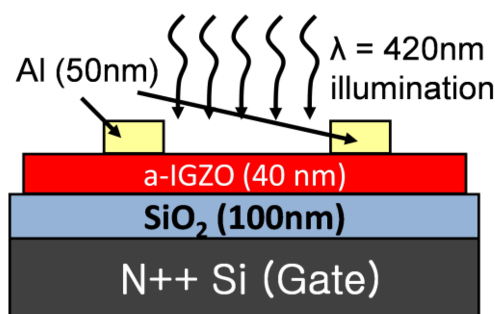

Fig. 1. Bottom gate a-IGZO TFT structure used in this study.

In this paper, we further explored the light intensity dependent TFT response along with the photofield-effect analysis. We presented, for the first time, the photofield-effect of the a-IGZO TFT under UV-monochromatic photo illumination that was used for extraction of the a-IGZO density-of-states (DOS).

2. Experimental

Fig. 1 shows a bottom gate a-IGZO TFT structure used in this study. A heavily doped (n^{++}) silicon wafer with 100 nm thermal oxide layer was selected as the gate electrode and insulator, respectively. A 40nm thick a-IGZO (In:Ga:Zn=1:1:1) active layer was deposited on the substrate by a pulse-laser deposition (PLD) system [4] and the deposition was done in an oxygen atmosphere without any intentional substrate heating. Before the source/drain electrodes deposition, a macro-island was formed by edge-dipping/etching of the substrate in dilute HCl solution. The 50nm thick aluminum (Al) source/drain electrodes were deposited through stencil mask openings by thermal evaporation. Finally, the device was thermally annealed in air at 300^0C for 5 minutes.

Electrical measurement of the a-IGZO TFT were

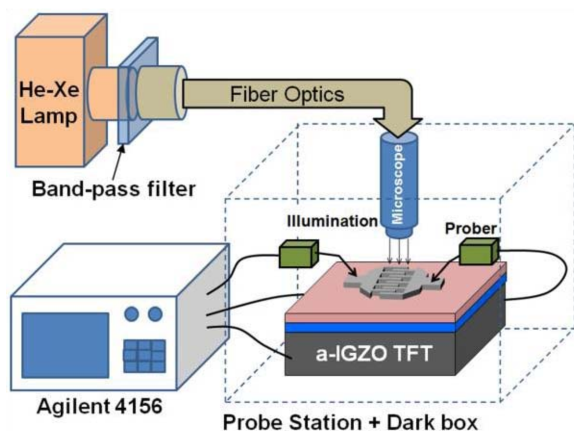

Fig. 2. The schematic of experimental setup used in this study

carried out with a probe station system located in a light tight box. The transistor electrical properties were measured by a PC controlled Agilent 4156 semiconductor parametric analyzer. During photofield effect measurement, photo excitation was provided by a He-Xe lamp in combination with narrow band filters and an optical fiber. The monochromic light passed through a fiber cable and probe station microscope, which is used to focus the illumination on the specific device. Fig. 2 shows the schematic of experimental setup used in this study. For each measurement, light intensity (irradiance, I ($\mu W/cm^2$)) was calibrated by Oriel 70260 radiant power meter with the photodiode sensor attached. All measurements were done at room temperature in ambient air. Optical absorption spectrum on a-IGZO thin film is also collected. At the UV wavelength that was chosen for this study (λ=420nm), our sample has absorption coefficient $\alpha \cong 714cm^{-1}$ which corresponds to an optical penetration depth ($\delta=1/\alpha$) of 14µm. Since δ is much larger than the thickness of the channel a-IGZO layer (40nm), the illumination is uniformly absorbed throughout the thickness during measurement.

3. Results and discussion

3.1 Dark TFT Electrical Properties

Saturation region TFT transfer characteristics were measured under dark. During drain current (I_{DS}) measurement, the drain voltage (V_{DS}) was set at 12V while the gate voltage (V_{GS}) was varied from -5~12V. Threshold voltage (V_{th}) and field-effect mobility (μ_{eff}) were extracted from the best linear fit (90~10%) of the $I_{DS}^{1/2}$-V_{GS} data and the standard MOSFET I_{DS} formula was used:

$$I_{DS} = \mu_{eff} C_{ox} \frac{W}{2L} (V_{GS} - V_{th})^2 \quad (1)$$

TABLE 1. Key TFT Electrical Properties

a-IGZO TFT (W/L=1040µm/35µm)					
	μ_{eff}	V_{th}	S	I_{DS_off}*	On/off ratio*
Unit	cm^2/Vs	V	V/decade	A	
Value	3.2	2.8	0.28	$<10^{-12}$	$>10^8$

* I_{DS_off} is the off-state drain-current and "on/off ratio" is the drain current ratio between on and off states.

where C_{ox} is gate insulator capacitance per unit area. The subthreshold swing (S) was also extract from TFT transfer characteristic in the subthreshold region, using the following equation:

$$S = \left(\frac{d \log(I_{DS})}{dV_{GS}} \right)^{-1} \quad (2).$$

Key TFT properties are further summarized in Table 1. They indicated our TFT has good electrical performance and is suitable for photofield-effect analysis.

3.2 TFT Electrical Properties under Illumination

We applied a monochromatic light (λ=420nm) to uniformly illuminate the TFT channel area directly through probe station microscope. The wavelength was chosen to match the absorption properties of the a-IGZO. Fig. 3 shows the TFT transfer characteristics measured under dark and with different irradiance levels (E) up to 10$\mu W/cm^2$. We further extracted TFT parameters for each individual level and plot them as a function of light intensity (Fig. 4). I_{DS_off} was found to increase with the illumination intensity, along with

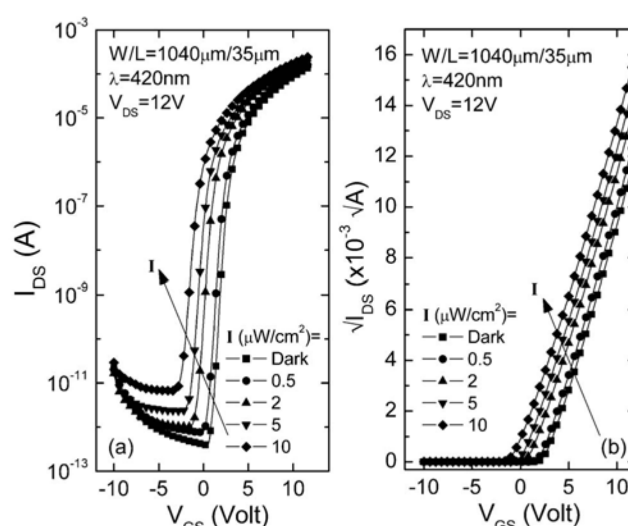

Fig. 3. a-IGZO TFT I_{DS}-V_{GS} curves for dark and different irradiance levels (I) in (a) semi-log plot and (b) linear plot.

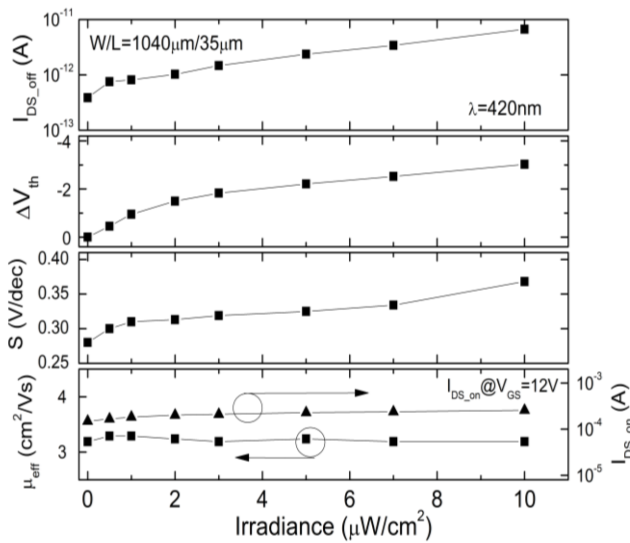

Fig. 4. Dependence of TFT I_{DS_off}, ΔV_{th}, S, μ_{eff} and on-current (I_{DS_on}) on the irradiance level.

a negative shift of threshold voltage (ΔV_{th}). S raises from 0.28 to 0.37 V/dec at I=10μW/cm^2. This is primarily due to the increase of I_{DS_off} and can be seen clearly under threshold voltage normalized transfer curves (Fig. 5). The μ_{eff} almost remains unchanged during this study. The result indicates a strong UV photon absorption in a-IGZO layer and electron-hole pairs generated by photo-excitation cause the bulk conductivity to increase. It is worthy to notice that the negative ΔV_{th} has also been observed in wavelength dependent photo-sensitivity study [3]. The device can return to its original dark states by baking at 100^{0}C for few minutes. With no applied heat, the device will regain its dark states after a much longer (days) period of time. We speculated that the charge trapping (one possibility is hole trapping) is responsible for ΔV_{th}. This was further supported by the fact that all the TFT transfer curves share the same threshold voltage normalized turn-on voltage (about -2V) as illustrated in Fig. 5.

3.3 Photofield-Effect Analysis

The photofield-effect theory was originally developed by Schropp *et al.* and later used to explain the photoconductivity under a controlled gate bias in a-Si:H TFT [5-7]. It was also successfully used to analyze the electrical properties under illumination in organic polymer TFT [8]. The analysis begins with the definition of photo-current (I_{ph}) as the difference between TFT drain current under illumination and dark:

$$I_{ph} = I_{DS_ill} - I_{DS_dark} \qquad (3).$$

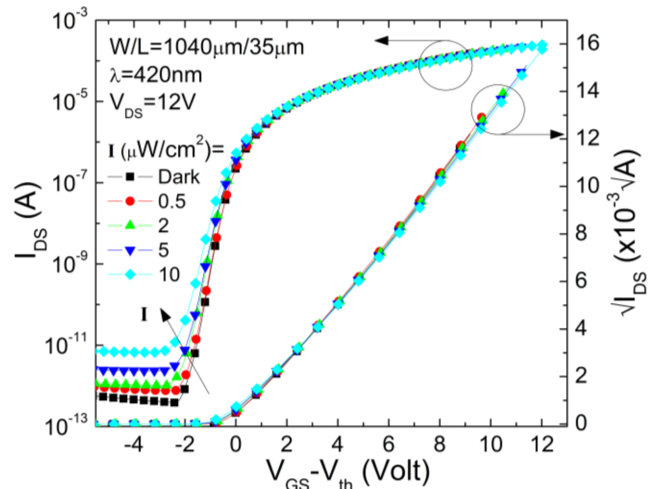

Fig. 5. Threshold voltage normalized (I_{DS} is plotted as a function of effective gate voltage, V_{GS}-V_{th}) a-IGZO TFT transfer properties for dark and different irradiance levels (I).

As illustrated in Fig. 6, the I_{ph} has power-law dependence (γ) with the irradiance level (I):

$$I_{ph} \propto I^{\gamma} \qquad (4)$$

and γ is a function of V_{GS}-V_{th}. Dash lines in Fig. 6 are linear fit for γ and it can be further described by an analytical theory.

The theory assumes a symmetrical overlap of the acceptor (N_A=N_f+αE) and donor (N_D=N_f - αE) states around mid-gap, where E is energy, N_f is a constant and α is the linear characteristic energy slope. Thus, the total density-of-states (DOS) around mid-gap (N_D+N_A =2N_f) is a constant.

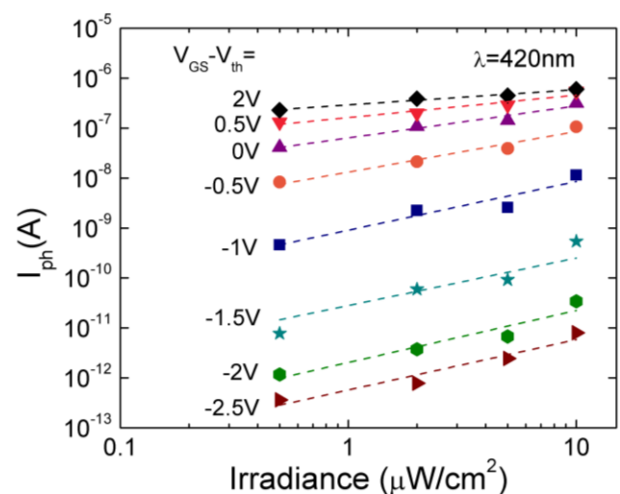

Fig. 6. Dependence of photocurrent (I_{ph}) on irradiance at various V_{GS}-V_{th} voltages. Dash lines are linear fits for power-law dependence coefficients gamma (γ).

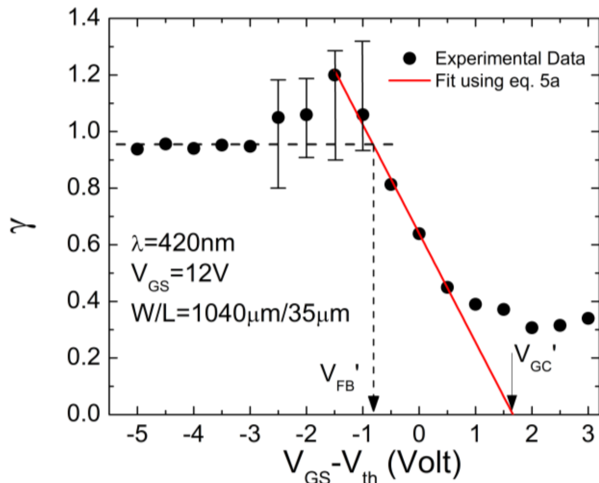

Fig. 7. Gamma factor (γ) of a-IGZO TFT versus V_{GS}-V_{th} at a wavelength of 420nm.

The dependence of γ on V_{GS}-V_{th} is given by following formulas:

$$\gamma = \begin{cases} \gamma_0 \left(1 - \frac{(V_{GS} - V_{th}) - V'_{FB}}{(V'_{GC} - V'_{FB})}\right), \ for\ (V_{GS} - V_{th}) > V'_{FB} & (5a) \\ \gamma_0 \qquad , \ for\ (V_{GS} - V_{th}) < V'_{FB} & (5b) \end{cases}$$

V_{FB}'=V_{FB}-V_{th_dark} and V_{GC}'=V_{GC}-V_{th_dark}. γ_0 is a material dependent constant. V_{FB} and V_{th_dark} are flat band voltage and dark threshold voltage, respectively. V_{GC} is also called critical voltage and is defined as:

$$V_{GC} = \frac{d_{ins}}{\varepsilon_{ins}} \left(\frac{\varepsilon_{semi}}{\varepsilon_0}\right)^{1/2} \frac{(2N_f)^{3/2}}{\alpha} \qquad (6)$$

where d_{ins} is the gate insulator thickness (=100nm), ε_{ins} and ε_{semi} are dielectric constants for gate insulator (3.9 for SiO_2) and a-IGZO (=10), respectively. Fig. 7 shows the γ extracted from Fig. 6 as a function of V_{GS}-V_{th} and the experimental data closely follow the analytical model (eq.5). The γ_0 is extracted to be near 1.0 which indicates that a-IGZO TFT is efficiently converting the UV-illumination to photocurrent in off-region. We then extracted the critical voltage (V_{GC}) and flat-band voltage (V_{FB}) to be 4.44V and 1.99V, respectively. In order to determine the mid-gap DOS characteristic slope α, we first determined the total mid-gap DOS, $2N_f$, by using the following formula [9]:

$$2N_f = \left(\frac{S \log(e)}{kT/q} - 1\right) \frac{C_{ox}}{q} \qquad (7)$$

where S is the TFT subthreshold swing. The $2N_f$ for our a-IGZO TFT is estimated to be ~10^{17} $cm^{-3}eV^{-1}$ which is consistent with what has been extracted using SPICE modeling [10]. By substituting all the parameters into eq.6, α is calculated to be 7.76×10^{16} $cm^{-3}eV^{-2}$. The extracted a-IGZO TFT mid-gap DOS is more than a order lower than the previously reported values for a-Si:H TFT [11]. The finding is supporting a good switching property of the a-IGZO TFTs that is experimentally observed.

4. Summary

In conclusion, we present a detail study on intensity dependent photo-response of the a-IGZO TFT under UV monochromatic illumination. By adapting the well developed photofield–effect theory, experimental data can be modeled and the a-IGZO mid-gap DOS properties were extracted. Compared to the a-Si:H TFT, a low subthreshold swing (S) in a-IGZO TFT is primarily due to a low mid-gap DOS. In addition, TFT photo-current is strongly proportional to the UV light intensity in off-region with a high photo-to-current conversion efficiency. This shows the potential for using a-IGZO TFT as UV-light photo-sensor / imager.

5. Acknowledgements

Two of the authors (T.C. Fung and J. Kanicki) would like to thank DARPA for their financial support during this work.

6. References

1. H. Hosono, *J. Non- Cryst. Solids,* **352**, 851-858, (2006).
2. A. Takagi, K. Nomura, H. Ohta, H. Yanagi, T. Kamiya, M. Hirano and H. Hosono, *Thin Solid Films*, **486**, 38-41 (2005).
3. C.-S. Chuang, T.-C. Fung, B.G. Mullins, K. Nomura, T. Kamiya, H.-P.D. Shieh, H. Hosono, and J. Kanicki, *SID 08 Digest*, 1215-1218 (2008).
4. K. Nomura, H. Ohta, A. Takagi, T. Kamiya, M. Hirano and H. Hosono, *Nature*, **432**, 488-492 (2004).
5. R.E.I. Schropp, G.J.M. Brouwer and J.F. Verwey, *J. Non-Cryst. Solids,* **77&78**, 511-514, (1985).
6. R.E.I. Schropp, T. Franke and J.F. Verwey, *J. Non- Cryst. Solids,* **90**, 199-202, (1987).
7. J.D. Gallezot, S. Martin and J. Kanicki, *Proc. IDRC, 2001*, 407-410.
8. M.C. Hamilton and J. Kanicki, *IEEE J. Select. Topics Quantum Electron.,* **10**, 840-848, (2004).
9. A. Rolland, J. Richard, J.-P. Kleider and D. Mencaraglia, *J. Electrochem. Soc.,* **140**, 3679-3683, (1993).
10 C. Chen, T.-C. Fung, K. Abe, H. Kumomi and J. Kanicki, *Proceeding of 66th Device Research Conference,* 151-152, (2008).
11. A. O. Harm, R.E.I. Schropp and J. F. Verwey, *Phil. Mag. B*, **52**, 59-70, (1985).